Geologia Sudetica, 2008, 40: 1–18.

Late-orogenic magmatism in the Central European Variscides: SHRIMP U-Pb zircon age constraints from the Żeleźniak intrusion, Kaczawa Mountains, West Sudetes

Katarzyna Machowiak[1], Richard Armstrong[2], Ryszard Kryza[3] & Andrzej Muszyński[4]

[1] *Institute of Civil Engineering, Poznań University of Technology, Piotrowo 5, 61-138 Poznań, Poland, e-mail: kamachow@amu.edu.pl*
[2] *Research School of Earth Sciences, The Australian National University, Canberra ACT 0200, Australia, e-mail: Richard.Armstrong@anu.edu.au*
[3] *Institute of Geological Sciences, University of Wrocław, Cybulskiego 30, 50-205 Wrocław, Poland, e-mail: ryszard.kryza@ing.uni.wroc.pl*
[4] *Institute of Geology, Adam Mickiewicz University, Maków Polnych 16, 61-606 Poznań, Poland, e-mail: anmu@amu.edu.pl*

Key words: Variscan igneous activity, geochemistry, zircon geochronology, Żeleźniak intrusion, West Sudetes.

Abstract We present new U-Pb isotope data obtained using the sensitive high mass-resolution ion microprobe (SHRIMP) technique on zircon crystals from the Żeleźniak subvolcanic intrusion in the Kaczawa Mountains, West Sudetes, SW Poland. The intrusion comprises shallow-level unmetamorphosed and undeformed fine-grained rhyolites, rhyodacites, and trachyandesites and deep-level medium-grained monzogranites and granodiorites. The surrounding country rocks, thought to be fragments of a Variscan accretionary prism, are blueschist- to subsequent greenschist facies metavolcanic and metasedimentary rocks of the Kaczawa Complex. The Żeleźniak intrusion has been correlated with other late- to post-tectonic Variscan volcanic and plutonic bodies in the region, such as the Karkonosze Granite, but the scarcity and often problematic quality of age constraints and of geochemical data have made such correlations speculative. Our new SHRIMP zircon ages of ~315–316 Ma from the Żeleźniak intrusion probably corresponds to the main magmatic stage. However, a younger age of ~269 Ma, derived from some zircon rims, is more difficult to interpret but might reflect either a much younger igneous event or a hydrothermal episode. The new date of ~315–316 Ma for the undeformed Żeleźniak intrusion also provides an upper age limit for deeper-level tectonic and metamorphic processes in the Kaczawa accretionary prism. Furthermore, the new SHRIMP zircon ages are among the oldest obtained from the volcanic rocks within the Variscan Belt in Central Europe and may correspond to the final stages of the exhumation of the blueschist facies rocks in this part of the orogen.

Manuscript received 16 May 2008, accepted 7 November 2008

INTRODUCTION

The pre-Permian geological evolution of central Europe is difficult to unravel but it is generally accepted that the basement structure of this area was largely formed during the Variscan "cycle" (*e.g.*, Mazur *et al.*, 2006 and references therein). However, the Variscan orogeny was obviously not a discrete event but a spectrum of long-lasting tectonic, magmatic and other, related, geological processes, that took place at different times in different places (*e.g.*, Aleksandrowski & Mazur, 2002). The structural mosaic of the basement units was finally shaped by late-orogenic tectonic displacements and sealed by widespread late-orogenic, and undeformed, Variscan granitoids during Carboniferous–Early Permian times. The granitic plutonism was accompanied by subvolcanic and volcanic activity, as recorded within time-equivalent Carboniferous and Lower Permian intramontane basin molasse successions (Mazur *et al.*, 2007).

The Variscan orogeny in the central European part of the orogenic belt started with the exhumation of deeply buried pre-Late Devonian crustal complexes, the age of these complexes being inferred from local, pre-Late-Devonian unconformities and from recently reported cooling ages (*e.g.*, Żelaźniewicz, 2003; Kryza *et al.*, 2004; Mazur *et al.*, 2006, and references therein).

The interpretation of the evolution of the Variscan orogen in the Sudetes has been helped by unraveling the relative ages of the Variscan igneous rocks – those that are syn-, late- and post-tectonic as defined by the presence of significant, weak or non-existant tectonic deformation, respectively – combined with their source affinities and

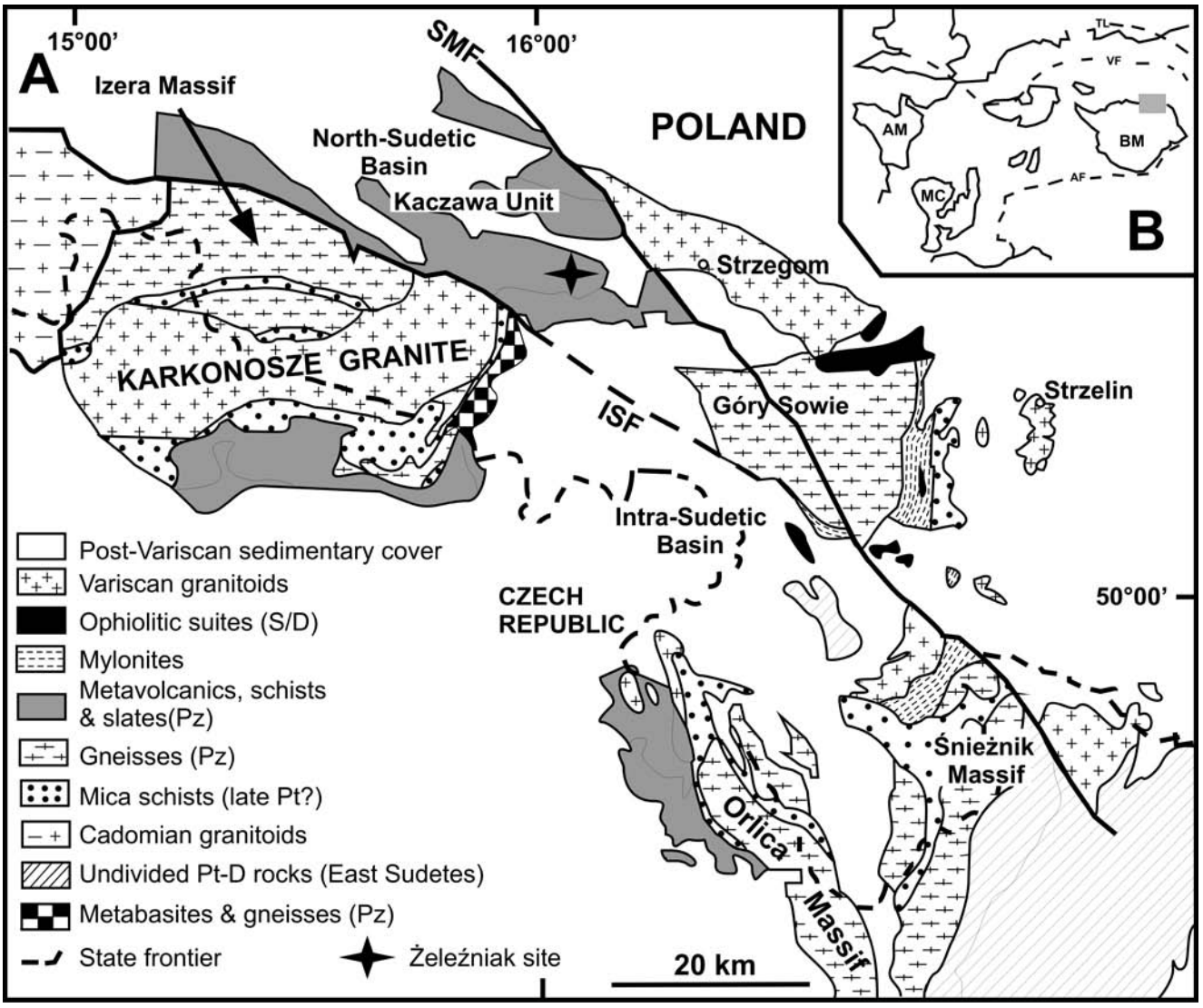

Fig. 1. (**A**) Geological map of the Sudetes (simplified after Aleksandrowski *et al.*, 1997). Abbreviations are as follows: C (Carboniferous); D (Devonian); ISF (Intra-Sudetic Fault); Pt (late Proterozoic); Pz (Palaeozoic); SMF (Sudetic Marginal Fault). (**B**) Inset map: Abbreviations are as follows: AF (Alpine Front); AM (Armorican Massif); BM (Bohemian Massif); MC (Massif Central); VF (Variscan Front); TL (Teisseyre–Tornquist Line).

structural positions. There is also significant variation among the ages of the Variscan granitoids of the Sudetes and Fore-Sudetic Block (Fig. 1): they vary from the Middle Devonian (~380 Ma) syn-tectonic granites, such as the anatectic granite dykes in the Góry Sowie Mountains (Timmermann *et al.*, 2000) or the Doboszowice orthogneiss in the Fore-Sudetic Block (Hanzl *et al.*, 1998), to the Upper Carboniferous/Lower Permian (~290–300 Ma) post-tectonic granites, such as the shallow-level Strzegom granites (Pin *et al.*, 1989; Turniak *et al.*, 2007 in press).

Intermediate Rb/Sr dates (*i.e.*, those falling between Early and Late Carboniferous times) are typical of the more widespread plutonic bodies: 347±12 Ma and 330±6 Ma for the Strzelin granites (Oberc-Dziedzic *et al.*, 1996), and 328±12 and 309±3 Ma for the Karkonosze Massif (Duthou *et al.*, 1991). The apparently corresponding predominantly acidic and/or bimodal volcanic rocks to these granites are found as shallow-level subvolcanic bodies in the basement complexes, as well as in the volcanic–sedimentary successions of the Intra-Sudetic- and North-Sudetic basins. The ages of the subvolcanic intrusives are uncertain, as are those of the volcanic rocks in the lowermost molasse deposits in the Intra-Sudetic Basin. Nevertheless, these molasse deposits are known to be diachronous, starting either with the Upper Devonian–Tournaisian coarse-clastic sediments of the Świebodzice- and Intra-Sudetic basins, or from the Stephanian red conglomerates in the North-Sudetic Basin (Awdankiewicz, 1999; Baranowski *et al.*, 1990). By contrast, the ages of the voluminous bimodal volcanic rocks that occur higher in the succession are relatively well constrained via palaeontological evidence derived from interbedded sedimentary rocks (Awdankiewicz, 1999, and references therein): these provide an Autunian age (~295–270 Ma).

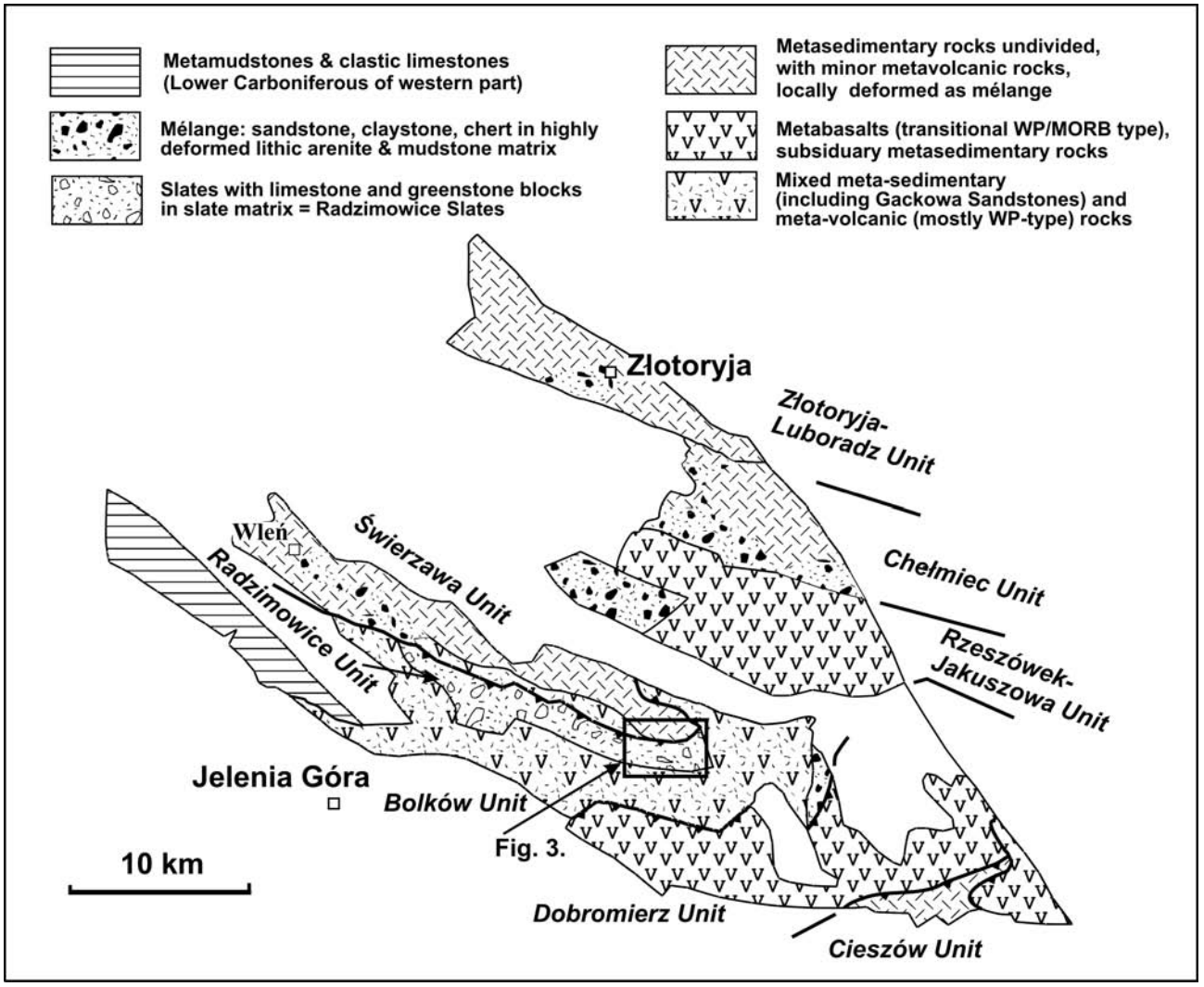

Fig. 2. Geological sketch map of the Kaczawa Mountains (after Baranowski *et al.*, 1990). Tectonic unit abbreviations are B (Bolków), Ch (Chełmiec), D (Dobromierz), R (Radzimowice), RJ (Rzeszówe–Jakuszowa), S (Świerzawa), ZL (Złotoryja–Luboradz). Other abbreviations are: ISF (Intra-Sudetic Fault), MSF (Marginal Sudetic Fault), NSB (North-Sudetic Basin). The box is the location of the study area shown in Fig. 3.

This paper presents SHRIMP U-Pb zircon ages from the Żeleźniak rhyolitic hypabyssal intrusion of the Kaczawa Mountains, ~15 km ENE of Jelenia Góra in SW Poland (Fig. 1). This is one of the largest late-orogenic, subvolcanic bodies of the Sudetes and it cuts the low-grade (blueschist- to greenschist facies) metamorphic rocks of the Kaczawa Complex. The Kaczawa Complex itself is composed of a ?Cambrian through Lower Carboniferous metavolcanic–metasedimentary succession and has been interpreted as part of a Variscan accretionary prism (Baranowski *et al.*, 1990; Kryza & Muszyński, 1992; Collins *et al.*, 2000). The age of the unmetamorphosed, undeformed, post-tectonic Żeleźniak intrusion is important not only to constrain the timing of regional metamorphism and the intense tectonic deformation of the Kaczawa Complex, which is unconformably covered by Stephanian (~300 Ma) and younger red clastic sediments, but also to correlate the Żeleźniak intrusion with the other Variscan igneous rocks in adjacent geological units, such as the Karkonosze Pluton and the Strzegom–Sobótka Massif.

GEOLOGICAL SETTING

The Żeleźniak intrusion is located in the central southern Kaczawa Mountains (Fig. 2) in the West Sudetes, ~3 km east of the town of Wojcieszów, and ~10 km NE of the Main Intra-Sudetic Fault across which the Kaczawa Complex is tectonically cut from the Karkonosze Pluton (Fig. 1). The Żeleźniak intrusion has an irregular star-like shape composed of a ~3 km^2 core, and a number of roughly radially arranged dykes that range from several metres to hundreds of metres in thickness and up to 7 km in length (Fig. 3). The acid subvolcanic rocks, mostly por-

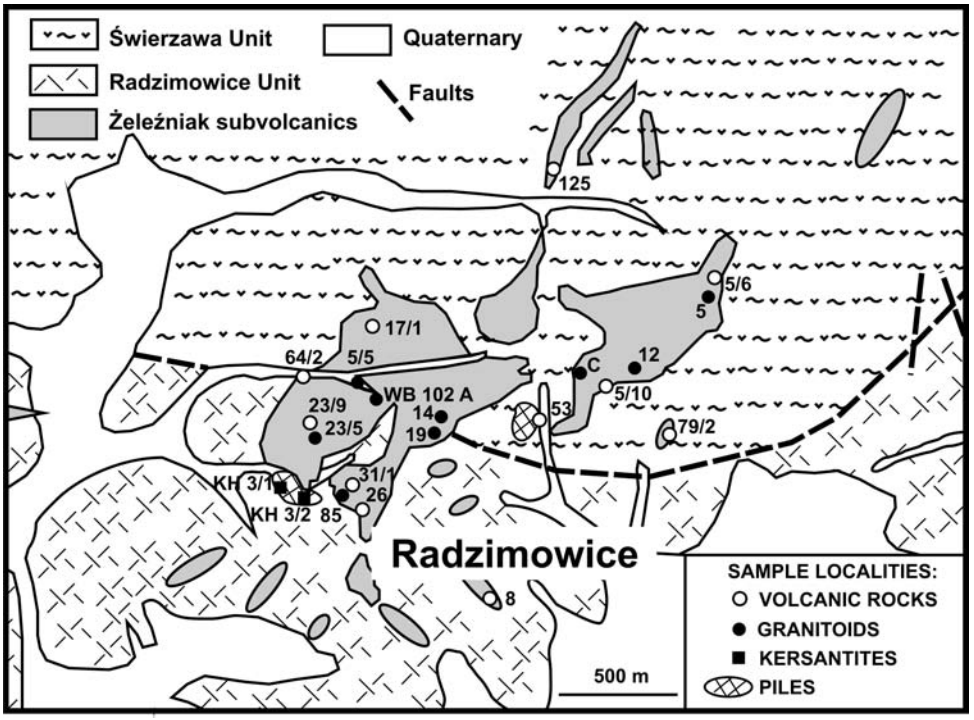

Fig. 3. Sketch map of the Żeleźniak intrusion and of the sample locations. The Świerzawa Unit comprises slates, diabases (dolerites), pillowed metabasalts, metatrachytes, and metasedimentary rocks. The Radzimowice Unit comprises slates and the Żeleźniak subvolcanic rocks. Quaternary sediments and recent alluvium have not been differentiated.

phyries or rhyolites, are rather common in the neighbouring areas where they are found mostly as dykes that follow the NNE–SSW trending faults in the metamorphic basement rocks of the Kaczawa Complex. Further to the north, similar felsic rocks form another subvolcanic body (the so-called "Organy Wielisławskie") and are an abundant member of the Lower Permian bimodal volcanic complex of the North-Sudetic Basin (Fig. 1).

The country rocks to the Żeleźniak intrusion are mostly the slates of the Radzimowice Unit (Kryza & Muszyński, 1992). This unit is itself in tectonic contact with two metavolcano-sedimentary successions: the slates, metadiabases, pillowed metabasalts, metatrachytes and metavolcaniclastic rocks of the more northerly Świerzawa Unit; and the so-called Wojcieszów Limestones, slates, metabasalts, metarhyodacites, metatrachytes and metavolcaniclastic rocks of the more southerly Bolków Unit. Evidence of an Early Palaeozoic age for the basement rocks comes from Cambrian macrofossils that have been confirmed from the Wojcieszów Limestones (Białek *et al.*, 2007); from conodonts, no older than the Ordovician, in the Radzimowice Slates (Urbanek & Baranowski, 1986); and from U-Pb zircon ages of ~485–500 Ma obtained from the metavolcanic rocks of the Świerzawa Unit (Kryza *et al.*, 2007, 2008).

The Żeleźniak intrusion has a distinct contact aureole up to several hundred metres wide in which relatively higher-grade thermal metamorphic minerals (*e.g.*, grossularite, diopside, hornblende-like amphibole, corundum and andalusite) overprint both the earliest blueschist facies and the later greenschist facies regional metamorphic assemblages (Kryza *et al.*, 1990).

PETROGRAPHY AND GEOCHEMICAL FEATURES

The spatial relationships between the different igneous facies of the Żeleźniak intrusion are obscure as a result of poor outcrop exposure and the difficulty posed to field mapping by the many disused mines in the region. Consequently, the remains of drill cores from the mining area have been of considerable value.

The igneous rocks of the Żeleźniak intrusion can be subdivided into two groups. Group 1 is a fine-grained subvolcanic facies. Group 2 is a medium-grained hypabyssal facies. The predominantly acidic and minor intermediate rocks of both groups are cut by subordinate, and apparently younger, kersantite dykes.

Group 1 comprises felsic rocks that display a variety of textures, including aphyric and porphyritic varieties, and that have mineral compositions corresponding to trachyandesites, rhyodacites, dacites and minor rhyolites (Fig. 4). The most common rock type is a trachyandesite that is, typically, a light-coloured, creamy- to pinkish-grey

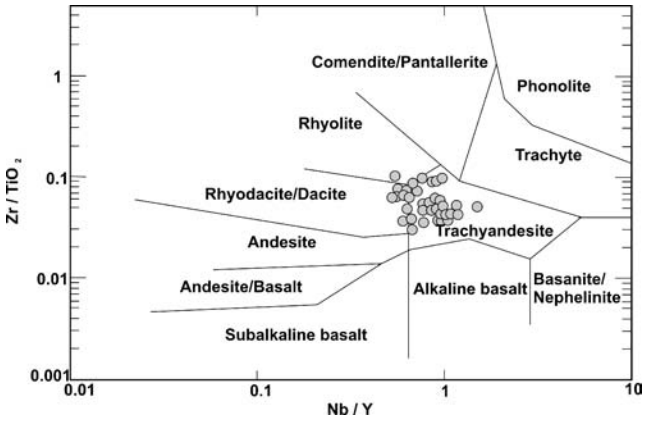

Fig. 4. The Żeleźniak volcanic rocks plotted on a Zr/TiO–Nb/Y diagram (after Winchester & Floyd, 1977).

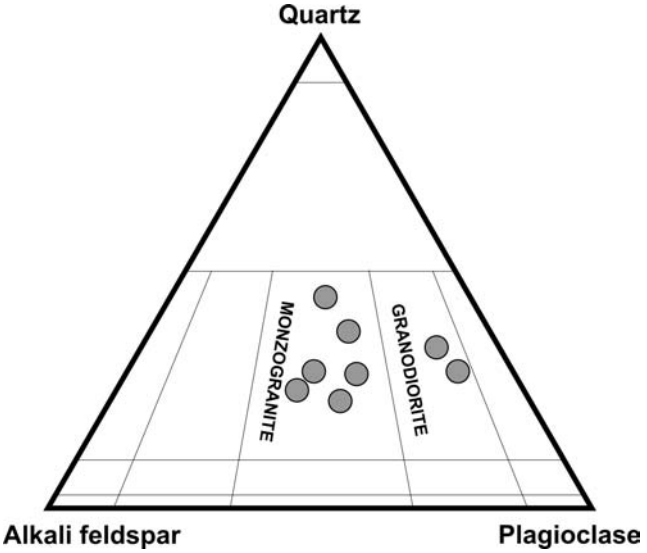

Fig. 5. Żeleźniak granitoids plotted on a quartz–alkali feldspar–plagioclase (QAP) diagram.

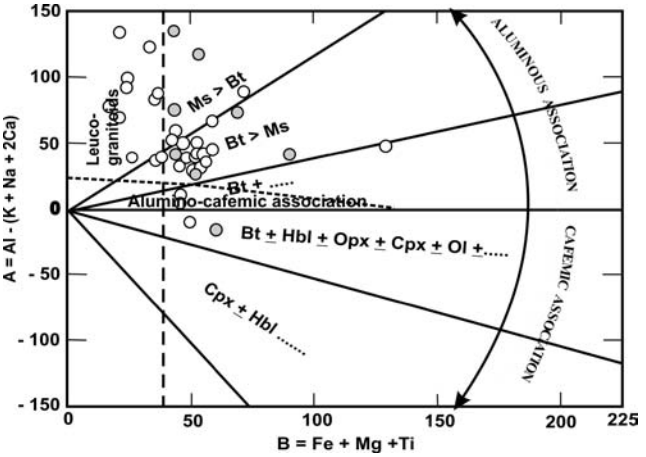

Fig. 6. Żeleźniak volcanic (open circles) and granitoid (full circles) rocks plotted on multicationic diagrams (after Debon & Le Fort, 1983).

rock with biotite and plagioclase phenocrysts, up to 0.5 cm in size. The groundmass is composed of quartz + K-feldspar + plagioclase intergrowths. The dacites and rhyodacites of Group 1 rocks contain embayed quartz phenocrysts, up to 0.7 cm in diameter, and fine-grained phenocrysts of plagioclase that are now strongly sericitized. Most of volcanic rocks of the Kaczawa Mountains are altered through sericitization, chloritization, kaolinitization, albitization and K-feldspathization.

Group 2 comprises relatively coarser-grained, commonly porphyritic, microgranitoids whose bulk mineral compositions plot within the fields of granites, monzogranites and granodiorites (Fig. 5). Most are biotite-bearing rocks, although one hornblende–biotite granite was found in a drill core. The microgranite is typically a light-grey, slightly pinkish rock of fine-grained and porphyritic texture, composed of plagioclase, quartz, biotite and usually subordinate K-feldspar. Also, one sample of a medium-grained granite from a drill core that reached a depth of 102 m contained hornblende and sphene (sample WB 102a, Fig. 3, Appendix 1).

The major- and trace-element chemistry and the Sr isotope characteristics of the Żeleźniak intrusion rocks were determined by Machowiak (2002). These results are given in Appendix 1, but the most important geochemical features can be summarized in the following 3 major points:

1. On a Zr/TiO_2–Nb/Y diagram (Fig. 4), the rocks of the Żeleźniak intrusion correspond to subalkaline magmas. Most samples are peraluminous, though a few are metaluminous (Figs. 5 and 6).

2. The rare earth element (REE) patterns of rocks representing the fine-grained facies (Group 1, three samples, Fig. 7) and the medium-grained facies (Group 2, five samples, Fig. 8) are broadly similar. They are characterized by rather low concentrations (7–10x chondrite), a flat distribution of heavy rare earth elements (HREE; from Eu to Lu), and have remarkably fractionated light rare earth element (LREE) distribution (~10x chondrite for Eu up to ~100–200x chondrite for La). In general, Group 1 rocks are considerably richer in LREE than rocks from Group 2. Worth stressing is that particular samples of medium-grained rocks from Group 2 display significantly different LREE/HREE enrichment (compare, for example, the relatively weakly enriched sample C, and rather strongly enriched sample 5/5 in Fig. 7), indicating possibly different sources or differentiation processes operating on the magmas. All the samples of both groups display either no or weakly negative Eu anomalies. The REE patterns of two kersantite samples (Fig. 8, samples KH3/1 and KH3/2) are broadly similar and resemble those of the microgranites.

3. The Sr isotope data (Machowiak, 2002) for 14 samples of the Żeleźniak intrusion, including the 2 kersantite specimens, display a surprisingly large variation (Table 1). The initial ratios of Sr and Nd isotopes in all the samples

Table 1

Sr and Nd isotope initial ratios, $^{0}\varepsilon Sr$ (caltulated to Sr = 0.7045, De Paulo 1988), and $^{0}\varepsilon Nd$ (calculated to Nd = 0.512638, Wasserburg *et al.*, 1981)

Sample	$^{143}Nd/^{144}Nd \pm$ Err	$^{87}Sr/^{86}Sr \pm$ Err	$^{0}\varepsilon$ Nd	$^{0}\varepsilon$ Sr
23/9 - rhyodacite	0.512252 ± 5	0.712611 ± 14	-7.5	115
79/2 - trachyandesite	0.512293 ± 8	0.711985 ± 12	-6.7	106
64/2 - rhyodacite	0.512260 ± 9	0.714943 ± 12	-7.4	148
26 - rhyodacite	0.512315 ± 7	0.717670 ± 10	-6.3	187
23/5 - monzogranite	0.512219 ± 6	0.728809 ± 14	-8.2	345
12 - monzogranite	0.512285 ± 8	0.718721 ± 15	-6.9	202
5 - monzogranite	0.512298 ± 6	0.710358 ± 13	-6.6	83
14 - monzogranite	0.512226 ± 8	0.715102 ± 17	-8.0	150
C - granodiorite	0.512403 ± 9	0.708563 ± 20	-4.6	58
85 - monzogranite	0.512306 ± 5	0.710709 ± 13	-6.5	88
5/5 - monzogranite	0.512293 ± 8	0.715587 ± 15	-6.7	157
WB102a - granodiorite	0.512326 ± 7	0.709310 ± 9	-6.1	68
KH3/2 - kersantite	0.512312 ± 6	0.709561 ± 14	-6.4	72
KH3/1 - kersantite	0.512347 ± 5	0.708797 ± 11	-5.7	61

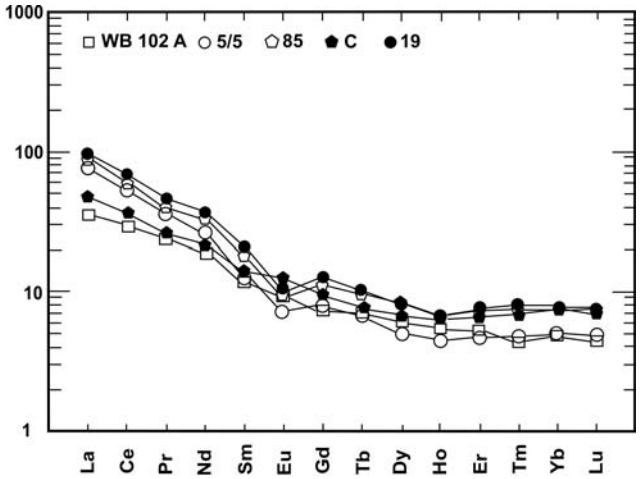

Fig. 7. Chondrite-normalized rare earth element (REE) plots of the Żeleźniak granitoids (normalized to values given in Nakamura, 1974).

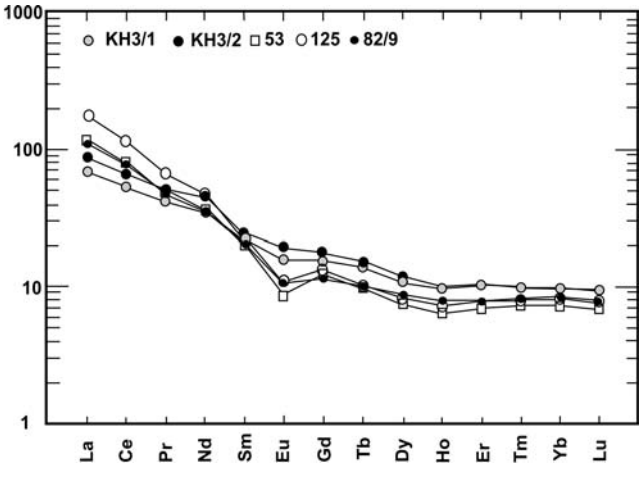

Fig. 8. Chondrite-normalized REE diagrams for the Żeleźniak kersantites (KH3/1 and KH3/2) and volcanic rocks (normalized to values given in Nakamura, 1974).

are typical of crustal values. The calculated $^{0}\varepsilon$ Nd < 0 and $^{0}\varepsilon$ Sr > 0 indicate either magma generated from continental crust or that had strong crustal contamination (Allègre & Othman, 1980). The high initial isotopic ratios and their wide variation indicate inhomogeneous crustal sources of the magmas (Johannes & Holtz, 1996), and confirm a composite character of the Żeleźniak intrusion, despite its relatively small size.

Plots of $^{87}Sr/^{86}Sr$ *vs*, 1/Sr (Fig. 9) suggest mixing of crustal magmas with material derived from a contaminated mantle source. Such trends may reflect a protolith evolved from mantle magmas that were subsequently involved in a recycling process (Faure, 2001).

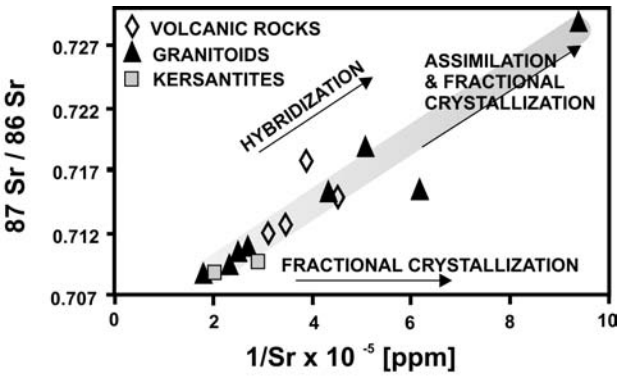

Fig. 9. Strontium isotopic data for the Żeleźniak subvolcanic rocks plotted on a Sr/Sr *vs*. 1/Sr diagram (after Faure, 2001).

ZIRCON DATING – SAMPLING AND ANALYTICAL METHODS

Of the five samples that were taken for zircon separation, two of them – sample 26 and sample 14 – were representative of the Group 1 and Group 2 facies, respectively, of the Żeleźniak intrusion and were selected for SHRIMP zircon dating.

Sample 26 is a rhyodacite of porphyritic texture, composed of microcrystalline matrix embedding phenocrysts of quartz, and of idiomorphic, weakly sericitized plagioclase, and fine-grained biotite. The sample was collected from the SW slope of Żeleźniak Hill.

Sample 14 is a monzogranite of fine- to medium-grained, slightly porphyritic texture, composed of quartz, plagioclase (oligoclase), K-feldspar, biotite, and accessory zircon and apatite. The sample comes from the central part of the intrusion (Fig. 3).

All five samples (0.5–2.0 kg) were crushed (®Pulverisette crusher) and sieved to obtain several grain-size fractions and accessory minerals were separated using magnetic and electromagnetic techniques. Zircons suitable for age determination (from samples 14 and 26) were manually separated under a binocular microscope. Other zircons for morphologic study were separated using sodium polytungstate [$Na_6(H_2W_{12}O_{40})H_2O$; density 3.0 g/cm^3] heavy liquid.

Zircon grains were mounted and polished to approximately half their thicknesses and photographed in both reflected and transmitted light. Cathodoluminescence (CL) and scanning electron microscope (SEM) images were prepared for all zircons and were used to decipher the internal structures of the sectioned grains and to target specific areas within the zircons for spot analysis.

All U-Pb analyses were done using the SHRIMP II instrument, each analysis consisting of 6 scans through the mass range. The data were reduced in a manner similar to that described by Williams (1998, and references therein), using the SQUID Excel Macro of Ludwig (2000). The Pb/U ratios were normalised relative to a value of 0.1859 for the $^{206}Pb/^{238}U$ ratio of the FC1 reference zircons, equivalent to an age of 1,099 Ma (Paces & Miller, 1989). Uncertainties given for individual analyses (ratios and ages) are at the one sigma level; however, the uncertainties in calculated weighted mean $^{206}Pb/^{238}U$ ages are reported at the 95% confidence level and include the errors in the standard calibration. Concordia plots and weighted mean age calculations were carried out using Isoplot/Ex (Ludwig, 1999).

For this paper, the U-Pb data are plotted on Tera-Wasserburg concordia plots, with the measured data plotted uncorrected for common Pb, as is the convention for SHRIMP U-Pb analyses on zircons of this age where even small common Pb corrections and low concentrations of ^{207}Pb can make calculation of $^{207}Pb/^{206}Pb$ ages very imprecise. In these plots, the data from a single age population will lie on a mixing line with the radiogenic Pb and the common Pb compositions as end-members. Those analyses with the lowest common Pb content will lie closest to the concordia curve. Radiogenic Pb-loss is indicated by the data spreading to the right of the radiogenic composition, and inheritance would plot to the left. For the Phanerozoic zircon, ages are calculated using the $^{206}Pb/^{238}U$ data, and for the Proterozoic and Archaean analyses, the $^{207}Pb/^{206}Pb$ data are used to calculate minimum ages. For the latter, common Pb corrections are made using the measured ^{204}Pb and the appropriate model Pb composition after Stacey and Kramers (1975). The $^{206}Pb/^{238}U$ dates are calculated from data corrected for common Pb using ^{207}Pb and assuming $^{206}Pb/^{238}U$– $^{207}Pb/^{235}U$ concordance.

RESULTS

GENERAL FEATURES OF THE ZIRCONS

Zircons from all 5 of the zircon-separation samples are usually euhedral or subeuhedral and colourless. The average crystal length is 230 μm (maximum 800 μm) and average breadth is 95 μm (maximum 220 μm). Following the typological method of Pupin and Turco (1972), 9 to 15 different zircon types were observed in individual samples. Most frequent among these are S_1, S_2, G_1, P_1, less frequent are S_{11}, S_{12}, P_2 and S_{21}. Inferred temperatures of crystallization of these zircon types are 650–700^0 °C and, rarely, 800–850^0 °C. The S_1 and S_2 types may have different origins/sources compared with the G_1 and P_1 types (crustal and mantle affinity, respectively; Pupin & Turco, 1972; Pupin, 1980; Pupin, 1988). Thus, the igneous rocks from the Żeleźniak intrusion appear to have a hybrid origin, which is supported both by zircon typology and by rock geochemistry.

MONZOGRANITE, SAMPLE 14

The zircons from sample 14 are clear, euhedral to subhedral and somewhat variable in form; morphologically, they are dominated by bipyramids with pronounced, sharp pyramidal tips (Fig. 10). Cathodoluminescence imaging showed the well developed, concentric compo- sitional zoning typically observed in zircons that have crystallised from a felsic magma. Occasional sector zoning and broad compositional zoning was observed in discrete crystals and within the central portions of some grains. Cathodoluminescence also showed the presence of a number of inherited zircon cores of variable size and shape. Although these were generally avoided during the analyses, a few were analysed to determine the pattern of inheritance in their host rocks.

Nineteen analyses were performed on 17 different zircons, the data from which are given in Appendix 2 and plotted as Tera-Wasserburg U-Pb concordia plots in Fig-

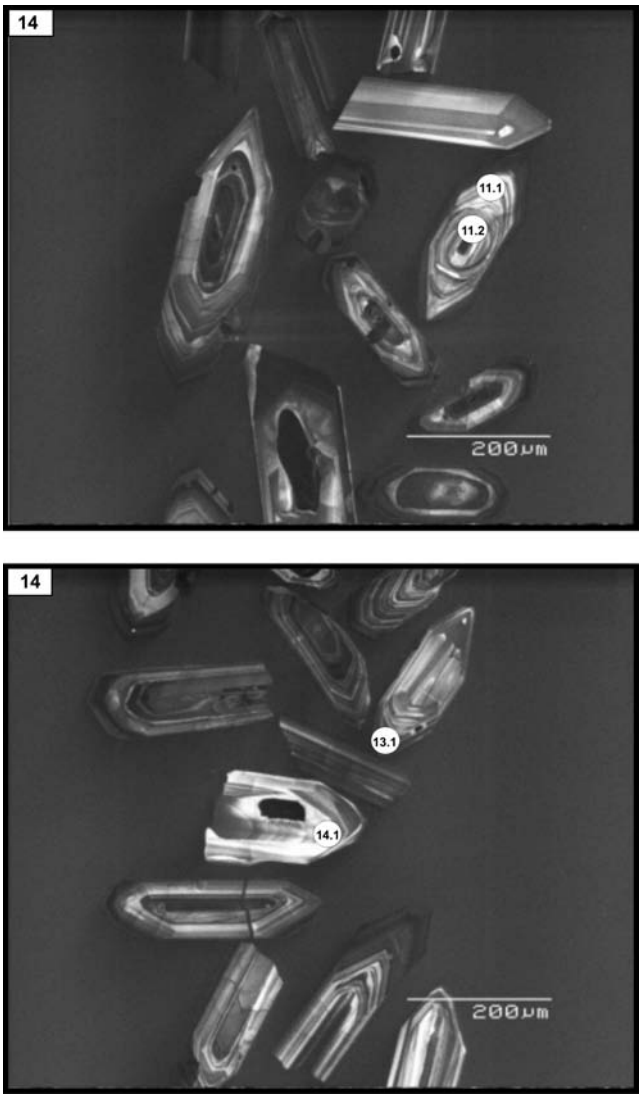

Fig. 10. Cathodoluminescence (CL) images of zircons from monzogranite (sample14). The numbers refer to the analyses listed in Appendix 2.

ure 11. Despite spots being selected to avoid very U-rich zones, most zircons had high (>500 ppm) U concentrations. A certain amount of discordance in some of the analyses is probably attributable to Pb-loss or to inheritance. Excluding these discordant data (points 5.1, 8.1, 10.1), thirteen analyses combine to give a weighted mean $^{206}Pb/^{238}U$ age of 316.7 ± 1.6 Ma (95% confidence level; MSWD = 0.90; probability of fit = 0.55). This age of 316.7 ± 1.6 Ma is interpreted to be the age of crystallization of this monzogranite.

Three analyses were excluded from the data set. Two analyses of cores gave minimum $^{207}Pb/^{206}Pb$ ages of 642 Ma (analysis 4.2) and 2,598 ± 5 Ma (analysis 11.2). Analysis 4.1 was of an overgrowth on the inherited core, also gave an older age than the presumed crystallisation age, and might be the result of a mixed analysis that incorporated a portion both of the core and of the magmatic overgrowth. Two other analyses (5.1 and 10.1) were rejected because they appeared to have suffered Pb-loss (Appendix 2).

RHYODACITE, SAMPLE 26

The zircons from sample 26 are clear, euhedral to subhedral and have many different forms ranging from acicular to fragments of larger, platey crystals. The zircons are structurally complex with cores of several generations and sizes. Most grains comprise a zoned, outer growth phase that rims a complexly zoned, clearly xenocrystic, zircon core (Fig. 12). Others have centres that could be interpreted as pseudo-cores, *viz*. simply an earlier phase of growth during the same magmatic event that produced the more highly zoned outer phase but that crystallized under different conditions. And although there can be a marked change in the style of zoning and there might be a small apparent structural discontinuity between the centre and rim, the age differences between centre and rim cannot be resolved. This is not an uncommon problem when characterizing and interpreting internal zircon zoning textures from felsic rocks (*e.g.*, Pidgeon *et al.*, 1998), and often it is only the *in situ* geochronological analyses that can resolve the issue if the age difference is significantly large.

Eighteen analyses were done on 17 different grains, with analyses sited in all observed types and forms of zircon in an attempt to establish the geochronological history of sample 26. Many grains have cores which are rounded, obviously inherited, and give a range of ages up to ~2.1 Ga. Many grains are made up predominantly of structural cores, and analyses sited in these areas appear to define a single U-Pb date that is interpretable as representing a single generation or population. Figure 13 illustrates that seven of these analyses plot close to concordia, showing their relatively low common Pb contents, and combine to give a $^{206}Pb/^{238}U$ age of 315.0 ± 2.1 Ma (95% confidence level; MSWD = 0.95; probability of fit = 0.46).

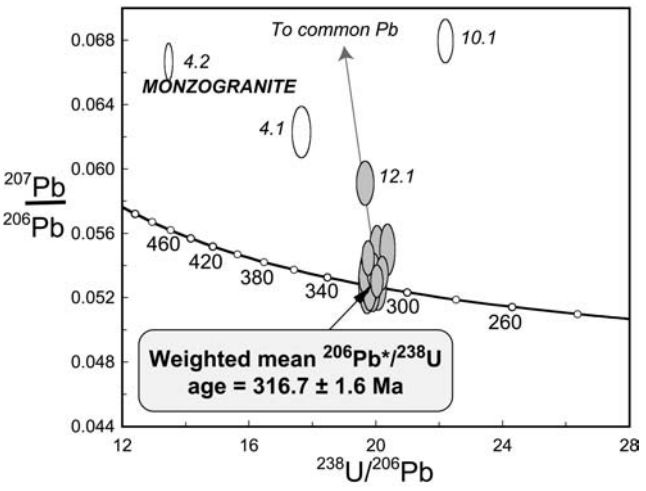

Fig. 11. Tera-Wasserburg U-Pb concordia plot of all the sensitive high mass-resolution ion microprobe (SHRIMP) data for the zircons from monzogranite (sample 14). The data are plotted uncorrected for common Pb.

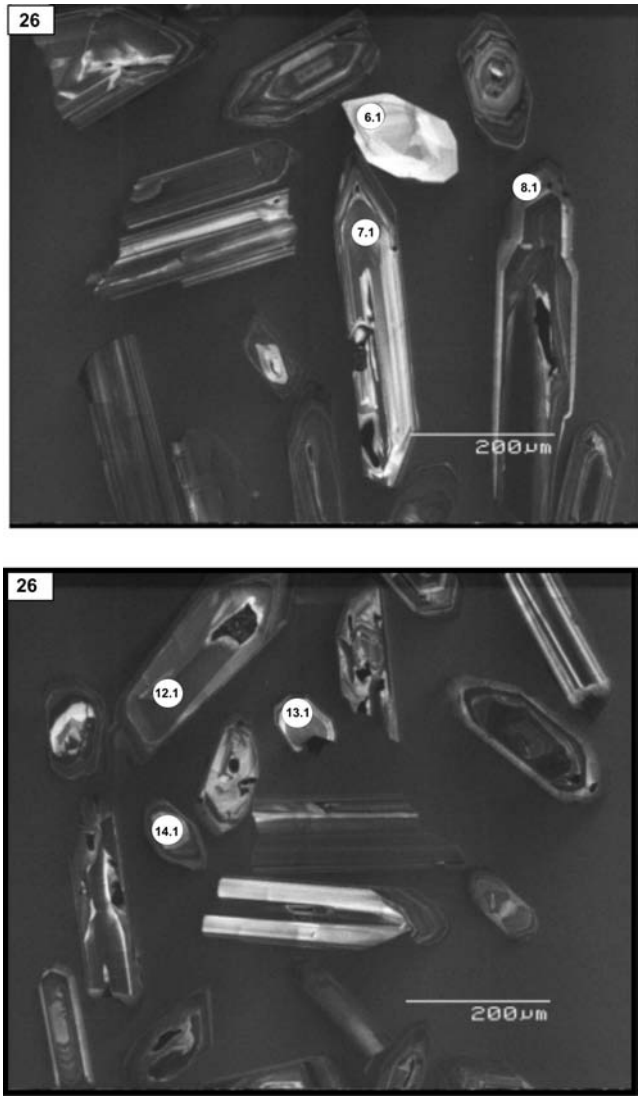

Fig. 12. Cathodoluminescence images of zircons from rhyodacite (sample 26). The numbers refer to the analyses listed in Appendix 3.

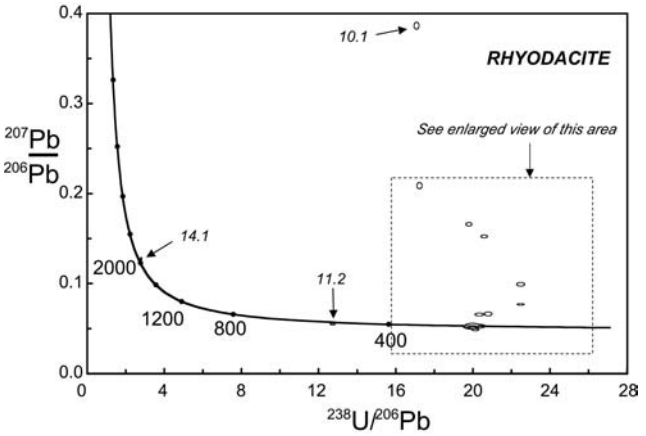

Fig. 13. Tera-Wasserburg U-Pb concordia plot of all the SHRIMP U-Pb data for the zircons from rhyodacite (sample 26). The data are plotted uncorrected for common Pb. An enlarged view of the outlined area is shown in Fig. 12.

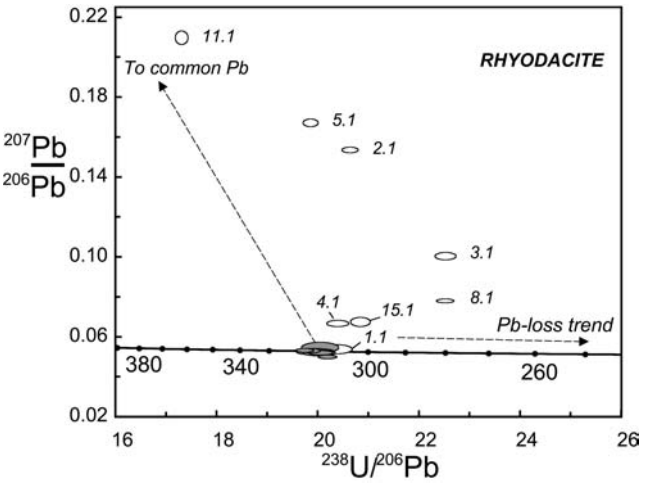

Fig. 14. An enlarged view of the Tera-Wasserburg U-Pb concordia plot of the SHRIMP U-Pb data for the zircons from rhyodacite (sample 26). The data are plotted uncorrected for common Pb. The error ellipses and labels are coloured according to the zircon type: zoned overgrowths are coloured black, the "cores" are coloured grey. White error ellipses represent data not included in the age calculations.

Three analyses (1.1, 4.1 and 15.1) on this type of zircon gave younger $^{206}Pb/^{238}U$ ages and appear to have suffered radiogenic Pb loss. The inclusion of analysis 1.1 in the above age calculation gives a weighted mean $^{206}Pb/^{238}U$ age of 314.5 ± 2.7 Ma, but a low probability-of-fit.

Five analyses of the highly zoned, euhedral outer margins of the grains show elevated, and variable, U and Th contents (Appendix 3). Unfortunately, these zones also have very high common Pb contents, with one analysis (10.1) having an extreme of 42% common ^{206}Pb (expressed as a percentage of the total ^{206}Pb). These high common Pb analyses plot far above the concordia curve in Figures 13 and 14. Four out of the five high common Pb analyses of this type (2.1, 3.1, 5.1 and 8.1) combine to give an apparent weighted mean $^{206}Pb/^{238}U$ date of 268.5 ± 4.0 Ma (95% confidence level; MSWD = 0.98; probability of fit = 0.40). The fifth analysis (11.1) has a higher apparent $^{206}Pb/^{238}U$ date and could be a mixed analysis. The significance of the date from the four-point analyses is uncertain, but it is possible that the clustering of these four points, which yields a reasonable weighted mean $^{206}Pb/^{238}U$ date, has a real age significance. Equally plausible is the possibility that these analyses are from altered or metamict zircon and, thus, have lost radiogenic Pb, resulting in a clustering of the age data that is simply fortuitous. High common Pb contents would be consistent with alteration.

SUMMARY OF RESULTS

Inheritance and Pb-loss complicate the data for both samples, with sample #26 (rhyodacite) being particularly difficult to interpret. The zircons from sample 14 (monzogranite), however, are clearly magmatic, and the magmatic age of this rock was determined by calculating the weighted mean $^{206}Pb/^{238}U$, which gave an age of 316.7 ± 1.6 Ma. Zircons from sample #14 also possessed inherited cores that gave ages as old as the Archaean.

The interpretation of the data for sample 26 (rhyodacite), however, is more difficult. Petrographic studies and cathodoluminescence imaging helped to identify a generation of zircon dated at ~315 Ma and to reveal older cores, all mantled by zoned high-U zircon with what could be interpreted as an apparently younger U-Pb age of about 269 Ma, albeit calculated from a small dataset. We propose that the ~315 Ma zircons represent the main magmatic population, possibly equivalent to that in the monzogranite (sample 14), and that the ~269 Ma overgrowths could represent a possible younger event, of either magmatic or fluid-induced metamorphic growth, or be the result of Pb-loss, the apparent $^{206}Pb/^{238}U$ dates having no geochronological significance. With regard to the first possibility, it is observed that the zircon overgrowths have high Th/U ratios (0.40–0.52), typical of magmatic zircons rather than those influenced by, or grown during, metamorphic and metasomatic processes. These latter processes typically produce zircons with Th/U < 0.1 (Pidgeon *et al.*, 1998; Schaltegger *et al.*, 1999; Eichhorn *et al.*, 1999). If these young zircon overgrowths really represent an igneous episode, then that event would correspond to the youngest Variscan plutonic/hypabyssal event dated thus far in the region and possibly be contemporaneous with middle Early Permian (Autunian) volcanic activity recorded in the Intra-Sudetic and North-Sudetic basins. However, these young zircon overgrowth ages, when considered in relation to the ~315 Ma age of the main intrusion, may simply reflect post-magmatic hydrothermal and metasomatic activities that could be part of the same event that led to the formation of the polymetallic lodes of Stara Góra (Mikulski, 2005).

The new SHRIMP results indicate that the main magmatic episode in the Żeleźniak intrusion, and the one that produced the main zircon populations, took place around 315 Ma (late Namurian). The ages of both the fine-grained rhyodacite and the medium-grained monzogranite are very similar, despite the observed petrographic, geochemical and Sr isotope complexity of the intrusion and despite the intense late-magmatic hydrothermal processes that also affected the body. Although our measurements did not concentrate on dating zircon cores, the few cores that were analysed suggest the presence of inherited grains that are up to ~2.6 Ga.

REGIONAL CORRELATIONS AND IMPLICATIONS

The Żeleźniak intrusion has been correlated with other bodies of generally undeformed igneous rocks in the region (Majerowicz & Skurzewski, 1987), and these igneous rocks are thought to have originated from late- to post-tectonic Variscan magmatic activity. However, scarce, and often problematic, age constraints, combined with insufficient geochemical data, have made such correlations speculative.

Manecki (1965), Paulo & Salamon (1974), and Majerowicz and Skurzewski (1987) have all suggested possible genetic links between the Żeleźniak intrusion and the Karkonosze pluton to the SW. Although the distance between the Żelaźniak intrusion and the Karkonosze pluton is only ~10 km, the two areas are separated by the Main Intra-Sudetic Fault, which cuts the thermal aureole of the pluton (Kryza & Mazur, 1998). This fact suggests that there have been tectonic displacements along this fault of several hundred metres at least, and possibly as much as a few kilometers to tens of kilometers (Aleksandrowski *et al.*, 1997).

Important for these correlations are recent petrological studies on the Karkonosze pluton by Słaby and Martin (2008). However, a general comparison of geochemical features between the Karkonosze granites and the Żeleźniak intrusives points to significant differences between the two intrusions (Machowiak, 2002). The Karkonosze granites display more distinct features of crustal magmas: higher contents of K_2O, Na_2O, Rb, Cs, Y, and lower concentrations of P_2O_3, CaO, Fe_2O_3, TiO_2 and Sr. These characteristics are further supported by trends on Harker diagrams and on REE plots (see Machowiak, 2002), the data indicating a mixed origin and an important role of fractional crystallization in the formation of the main types of the Karkonosze granites (Słaby & Martin, 2008). Also, on trace element discrimination diagrams of the type in Pearce *et al.* (1984), the Karkonosze granites plot mostly in the fields of syn-collisional and within-plate granites, whereas those from Żeleźniak correspond to volcanic arc granites. These chemical differences, however, reflect somewhat different magma sources and/or differentiation (fractionation/contamination) processes rather than significantly different emplacement settings of these, roughly contemporaneous, felsic magmas.

The Karkonosze Granite has been difficult to date precisely: published dates vary between ~304 (Kusiak *et al.*, 2008) and 328 Ma (Duthou *et al.*, 1991) (Table 2). SHRIMP zircon dating of a microgranodiorite dyke that cuts the granite yielded an age of ~318 Ma (Awdankiewicz *et al.*, 2009). This would constrain the age of the hypabyssal magmatism in the Karkonosze Massif, as well as the minimum age of the Karkonosze Granite in that part of the pluton. Such an age is in broad agreement, within error, of

Table 2

Selected granitoids of SW Poland and their isotopic ages

Intrusion	Rock types	Ages (methods)	Data sources
Karkonosze	Porphyritic granite Porphyritic granite Even-grained granite	328 ± 12 (Rb-Sr) 329 ± 17 (Rb-Sr) 309 ± 3 (Rb-Sr)	Duthou *et al.*, 1991
Karkonosze	Medium-grained porphyritic granite Coarse-grained porphyritic granite Even-grained granite (Miedzianka)	314.1 ± 3.3 (U-Pb zircon, SHRIMP) 318.5 ± 3.7 (U-Pb zircon, SHRIMP) 314.9 ± 4.5 (U-Pb zircon, SHRIMP)	Machowiak & Armstrong, 2007
Karkonosze	Medium-grained porphyritic granite Coarse-grained porphyritic granite Fine-grained equigranular granite	313.0 ± 6.0 (U-Pb zircon, SHRIMP) 308.7 ± 4.7 (U-Pb zircon, SHRIMP) 303.7 ± 6.6 (U-Pb zircon, SHRIMP)	Kusiak *et al.*, 2008
Karkonosze	Micromonzodiorite dyke	318 ± 3 (U-Pb zircon, SHRIMP)	Awdankiewicz *et al.*, 2009, in press
Strzegom-Sobótka	Hbl-Bt monzogranite Two-mica monzogranite	278 ± 7 (Rb-Sr) 326 ± 22 (Rb-Sr)	Pin *et al.*, 1989
Strzegom-Sobótka	Bt-monzogranite Hbl-Bt monzogranite	308.4 ±1.7 (Pb-evaporation zircon) 302.9 ±2.2 (Pb-evaporation zircon)	Turniak *et al.*, 2005
Strzegom-Sobótka	Bt-monzogranite Hbl-Bt monzogranite	294.2 ±4.3 (K-Ar) 298.7 ±5.2 (K-Ar) 291.0 ±4.4 (K-Ar)	Turniak *et al.*, 2007
Strzelin I (Gębczyce)	Fine-grained granite	330 ± 6 (Rb-Sr) 347 ± 12 (Rb-Sr)	Oberc-Dziedzic *et al.*, 1996
Strzelin II (Lipowe Hills)	Fine-grained granite	329 ± 11 (Rb-Sr)	Oberc-Dziedzic et al. 2000
Strzelin	Tonalite Biotite granite	291 ± 5,5 (Pb-evaporation zircon) 301 ± 7 (Pb-evaporation zircon)	Turniak, 2006

earlier Rb–Sr dating of the main (porphyritic) granite facies of the Karkonosze pluton at 328 ± 12 Ma (Duthou *et al.*, 1991) and with the more recent SHRIMP zircon ages of 318.5 ± 3.7 Ma for the porphyritic granite of the NE part of the same pluton (Machowiak & Armstrong, 2007). Similarly "old" ages have recently been confirmed by refined SHRIMP dating using chemically abraded zircons (R. Kryza T. Oberc-Dziedzic, C. Pin, 2008, unpublished).

Our new age of ~315 Ma for the Żeleźniak intrusion is slightly younger than the ~320 Ma age of the main granite type of the Karkonosze pluton (Table 2). However, the dates do overlap within analytical error. The even-grained facies of the Karkonosze Granite might be younger at 309 ± 3 Ma (Duthou *et al.*, 1991), but this younger age needs further verification.

Possible direct genetic links with more distant granitic plutons of the region remain even more uncertain when one takes into account tectonic limitations and that many previous isotopic analyses suffered from a lack of precision. The Strzegom–Sobótka Massif has its western margin ~18 km ENE of the Żeleźniak intrusion and is the second largest granitoid pluton in the region. It is composed of at least three major parts (Table 2): (1) a hornblende–biotite monzogranite in the west; (2) a two-mica monzogranite in the center; (3) a biotite-granodiorite in the east (Majerowicz, 1972). The Rb–Sr whole rock isochron ages for the Strzegom–Sobótka granites indicate that the two mica monzogranite is considerably older (326 ± 22 Ma) than both the Hbl–Bt monzogranite and the Bt-granodiorite and that the latter two granite types display similar ages of about 280 Ma (Table 2; Pin *et al.*, 1989). The age of the older two-mica central part of the massif corresponds roughly, within error, to the ~315 Ma age of the Żeleźniak intrusion, whereas the younger (280 ± 10 Ma) part of the massif is not much older than the youngest age (268.5 ± 3.9 Ma) obtained for the Żeleźniak intrusion. However, recent zircon dating by the Pb-evaporation method (Turniak *et al.*, 2007) yielded very different ages for the main granite facies in the Strzegom–Sobótka Massif: between ~303 and 308 Ma (Table 2). These ages are in obvious conflict with previous dates and make precise correlations difficult.

Taking into account all previous age data (Table 2), attempting to correlate the Żeleźniak intrusion with more distant granitoid bodies is even more speculative. To do this, one would require more detailed and reliable ages from all the granitoids of the Sudetes: this applies to Rb–Sr data and to the still rather scarce, and in some cases problematic, U-Pb data.

The ~315 Ma age of the hypabyssal Żeleźniak intrusion may broadly correspond with Upper Carboniferous (Namurian–?Westphalian) subvolcanic and volcanic bodies of felsic rocks in the Intra-Sudetic Basin (*e.g.*, the Chełmiec intrusion west of Wałbrzych). However, the latter rocks have not yet been dated.

In a wider regional context, the ~315 Ma ages derived from the main population of magmatic zircons are among the oldest ages from the Variscan volcanic/subvolcanic rocks in this part of Europe, although similar ages of 297 ± 3 Ma to 302 ± 3 Ma have been reported from NE Ger-

many (Breitkreuz & Kennedy, 1999). Based on the available data, it is difficult to interpret the problematic younger dates on the zircon rims that gave a weighted mean $^{206}Pb/^{238}U$ date of 268.5 ± 4.0 Ma. If this really reflects a magmatic age, it would follow that the subvolcanic activity in the area lasted for (or was repeated) around 50 Ma after the main magmatic episode. This possibility seems to be supported by the prolonged volcanic records in the molasse sequences of the intramontane basins in the region (Awdankiewicz, 1999).

The new ages of ~315 Ma for non-metamorphosed and undeformed subvolcanic intrusion are also important for timing the deeper-level tectonic and metamorphic processes in this part of the Kaczawa Complex, which is thought to represent fragments of the Variscan accretionary prism (Baranowski *et al.*, 1990; Collins *et al.*, 2000; Kryza & Muszyński, 2003). The country rocks of the Żeleźniak shallow-level intrusion had previously gone through blueschist-facies and subsequent greenschist-facies metamorphism, probably significantly earlier than the intrusions and, evidently, at much deeper levels than the emplacement of the subvolcanic bodies themselves. Consequently, our new SHRIMP zircon age of ~315 Ma may be the upper age limit for the major exhumation processes that brought the deeply buried parts of the Kaczawa accretionary prism, including the glaucophane schists, to shallower crustal levels.

Acknowledgements

We acknowledge with thanks grants from the KBN (Polish Committee of Research; grants 6P04D 034 14 and 6PO4D 005 20) and from Wrocław University (grant 1017/S/ING/03-II). We thank Dr. C. Paquette and Dr. J.-P. Liégeois for their comments on an earlier version of this paper.

REFERENCES

ALLÈGRE, C. J. & OTHMAN, D. B., 1980. Nd–Sr isotopic relationship in granitoid rocks and continental crust development: a chemical approach to orogenesis. *Nature*, 286: 335–342.

ALEKSANDROWSKI, P., KRYZA, R., MAZUR, S. & ŻABA, J., 1997. Kinematic data on major Variscan strike-slip faults and shear zones in the Polish Sudetes, northeast Bohemian Massif. *Geological Magazine*, 134/5: 727–739.

ALEKSANDROWSKI, P. & MAZUR, S., 2002. Collage tectonics in the northeasternmost part of the Variscan Belt: the Sudetes, Bohemian Massif. *In*: Winchester J. A., Pharaoh, T. C. & Verniers, J. (Eds.), *Palaeozoic Amalgamation of Central Europe.* Geological Society of London, Special Publication, 201: 237–277.

AWDANKIEWICZ, M., 1999. Volcanism in the late Variscan intramontane trough: Carboniferous and Permian volcanic centers of the Intra-Sudetic Basin, SW Poland. *Geologia Sudetica*, 32, 1: 13–47.

AWDANKIEWICZ, M., AWDANKIEWICZ, H., KRYZA, R. & RODIONOV, N., 2009. SHRIMP zircon study of a micromonzodiorite dyke in the Karkonosze Granite, Sudetes (SW Poland): age constraints for late Variscan magmatism in Central Europe. *Geological Magazine* (in press).

BARANOWSKI, Z., HAYDUKIEWICZ, A., KRYZA, R., LORENC, S., MUSZYŃSKI, A., SOLECKI, A. & URBANEK, Z., 1990. Outline of the geology of the Góry Kaczawskie (Sudetes, Poland). *Neues Jahrbuch für Geologie und Paläontologie, Abhandlungen*, 179, 2–3: 223–257.

BIAŁEK, D., RACZYŃSKI, P., SZTAJNER, P. & ZAWADZKI, D., 2007: Archeocjaty wapieni wojcieszowskich. [*Archeocyata from the Wojcieszów Limestones.*] *Przegląd Geologiczny*, 55, 12/2, {in Polish, English summary}.

BREITKREUZ, C. & KENNEDY, A., 1999. Magmatic flare-up at the Carboniferous/Permian boundary in the NE German basin revealed by SHRIMP zircon ages. *Tectonophysics*, 302: 307–326.

COLLINS, A., KRYZA, R. & ZALASIEWICZ, J. A., 2000. Macrofabric fingerprints of Late Devonian-Early Carboniferous subduction in the Polish Variscides, the Kaczawa complex, Sudetes. *Journal of the Geological Society, London*, 157: 283–288.

DEBON, F. & LE FORT, P., 1983. A chemical-mineralogical classification of common plutonic rocks and associations. *Transactions of the Royal Society Edinburgh: Earth Sciences*, 73: 135–149.

DePAOLO, D. J., 1988. Neodymium isotope geochemistry. Springer Verlag (Berlin), pp. 187.

DUTHOU, J. L., COUTURIE, J. P., MIERZEJEWSKI, M. P. & PIN, C., 1991. Oznaczenia wieku granitu Karkonoszy metodą izochronową rubidowo-strontową, na podstawie całych próbek skalnych. [Dating of granite from the Karkonosze Mountains using the Rb–Sr total rock isochron method]. *Przegląd Geologiczny*, 36, 2: 75–79, {in Polish, English summary}.

EICHHORN, R., HÖLL, R., LOTH, G. & KENNEDY, A., 1999. Implications of U-Pb SHRIMP zircon data on the age and evolution of the Felbertal tungsten deposit (Tauern Window, Austria). *International Journal of Earth Sciences*, 88: 496–512.

FAURE, G., 2001. *Origin of igneous rocks. The isotopic evidence.* Springer (Berlin, Heidelberg), pp. 560.

HANZL, P., MAZUR, S., MELICHAR, R. & BURIANKOVA, K., 1998. Geochemistry of the Doboszowice orthogneiss and its correlation with rocks of the Silesicum and Moravicum. *Mineralogical Society of Poland, Special Papers*, 11: 100–103.

JOHANNES, W. & HOLTZ, F., 1996. Petrogenesis and experimental petrology of granitic rocks. Springer (Berlin, Heidelberg), pp. 335.

KRYZA, R., & MAZUR S., 1998. A strike-slip boundary between two HP low-grade metamorphic complexes in the West Sudetes (NE Bohemian Massif). *Acta Universitatis Carolinae: Geologica*, 42/2: 292–293.

KRYZA, R., MAZUR, S., ALEKSANDROWSKI, P., ZALASIEWICZ J. A., SERGEEV, S. & PRESNYAKOV, S., 2007. Early Palaeozoic initial-rift volcanism in the Central European Variscides (the Kaczawa Mountains, Sudetes, SW Poland): evidence from SIMS dating of zircons. *Journal of the Geological Society, London*, 164, 1207–1215.

KRYZA, R., MAZUR, S., OBERC-DZIEDZIC, T., 2004. The

Sudetic geological mosaic: Insights into the root of the Variscan orogen. *Przegląd Geologiczny*, 52, 8/2: 761–773.

KRYZA, R. & MUSZYŃSKI, A., 1992. Pre-Variscan volcanic-sedimentary succession of the central southern Góry Kaczawskie, SW Poland: Outline geology. *Annales Societatis Geologorum Poloniae*, 62: 117–140.

KRYZA, R. & MUSZYŃSKI, A., 2003. Kompleks metamorficzny Gór Kaczawskich – fragment waryscyjskiej pryzmy akrecyjnej. [The metamorphic Kaczawa Complex – fragment of a Variscan accretionary prism.] *In*: Ciężkowski W., Wojewoda J., Żelaźniewicz A. (Eds), *Sudety Zachodnie: od wendu do czwartorzędu.* WIND, Wrocław: 95–104, {in Polish, English summary}.

KRYZA, R., MUSZYŃSKI, A. & VIELZEUF, D., 1990. Glaucophane-bearing assemblage overprinted by greenschist-facies metamorphism in the Variscan Kaczawa complex, Sudetes, Poland. *Journal of Metamorphic Geology*, 8: 345–355.

KRYZA, R., ZALASIEWICZ, J. & RODIONOV, N., 2008. Enigmatic sedimentary-volcanic successions in the Central European Variscides: a Cambrian/Early Ordovician age for the Wojcieszów Limestone (Kaczawa Mountains, SW Poland) indicated by SHRIMP dating of volcanic zircons. *Geological Journal*, 43: 415–430.

KUSIAK, M. A., DUNKLEY, D. J., SŁABY, E., BUDZYŃ, B. & MARTIN, H., 2008. U-Pb chronology of zircon from granites of the Karkonosze Pluton, NE Bohemian Massif. *The 2008 SHRIMP Workshop, St. Petersburg, Russia*, Abstract Volume: 78–80.

LUDWIG, K. R., 1999. Isoplot/Ex version 2.00: A Geochronological Toolkit for Microsoft Excel. *Berkeley Geochronology Center Special Publication, 1a*, Berkeley, California, pp. 46.

LUDWIG, K. R., 2000. SQUID 1.00, A User's Manual. *Berkeley Geochronology Center Special Publication, 2*, Berkeley, California, pp. 17.

MACHOWIAK, K., 2002. Petrologia i wiek skał magmowych rejonu Żeleźniaka w Górach Kaczawskich. Petrology and age of igneous rocks in the area of Żeleźniak Hill (The Kaczawa Mts., Sudetes). Ph.D. thesis. Institute of Geology UAM Poznań, pp. 136, {in Polish, English summary}.

MACHOWIAK, K. & ARMSTRONG, R., 2007. SHRIMP U-Pb zircon age from the Karkonosze granite. *Mineralogia Polonica, Special Papers*, 31: 193–196.

MAJEROWICZ, A., 1972. Masyw granitowy Strzegom–Sobótka. Studium petrologiczne. [The Strzegom–Sobótka granitic massif. A petrological study] *Geologia Sudetica*, 6: 7–96, {in Polish, English summary}.

MAJEROWICZ, A. & SKURZEWSKI, A., 1987. Granity z okolic Wojcieszowa w Górach Kaczawskich. [Granites from the vicinity of Wojcieszów in the Kaczawskie Mountains.] *Acta Universitatis Wratislaviensis, Prace Geologiczno-Mineralogiczne*, 10 (788): 69–89, {in Polish, English summary}.

MANECKI, A., 1965. Studium mineralogiczno-petrograficzne polimetalicznych żył okolic Wojcieszowa (Dolny Śląsk). [Mineralogical and petrographical study of ore veins of the vicinity of Wojcieszów (Lower Silesia).] *Prace Mineralogiczne Komisji Nauk Mineralogicznych PAN Oddział w Krakowie*, 2: 7–58, {in Polish, English summary}.

MAZUR, S., ALEKSANDROWSKI, P., KRYZA, R. & OBERC-DZIEDZIC, T., 2006. The Variscan Orogen in Poland. *Geological Quaterly*, 50: 89–118.

MAZUR, S., ALEKSANDROWSKI, P., TURNIAK, K. & AWDANKIEWICZ, M., 2007. Geology, tectonic evolution and Late Palaeozoic magmatism of Sudetes – an overview. *In*: Kozłowski, A. & Wiszniewska, J., (Eds), *Granitoids in Poland*. Polish Geological Institute, Warszawa: 59–88.

MIKULSKI, S. Z., 2005. Geological, mineralogical and geochemical characteristics of the Radzimowice Au–As–Cu deposit from the Kaczawa Mountains (Western Sudetes, Poland): an example of the transition of porphyry and epithermal style. *Mineralium Deposita*, 39: 904–920.

NAKAMURA, N., 1974. Determination of REE, Ba, Fe, Mg, Na and K in carbonaceous and ordinary chondrites. *Geochimica et Cosmochimica Acta*, 38: 757–773.

OBERC-DZIEDZIC, T., PIN, C., 2000. The granitoids of the Lipowe Hills (Fore-Sudetic Block) and their relationship to the Strzelin granites. *Geologia Sudetica*, 33: 17–22.

OBERC-DZIEDZIC, T., PIN, C., DUTHOU, J. L. & COUTURIE, J. P., 1996. Age and origin of the Strzelin granitoids (Fore-Sudetic Block, Poland): Rb / Sr data. *Neues Jahrbuch für Mineralogie, Abhandlungen*, 171: 187–198.

PACES, J. B. & MILLER, J. D., 1989. Precise U-Pb ages of Duluth Complex and related mafic intrusions, Northeastern Minnesota: Geochronological insights to physical, petrogenic, paleomagnetic and tectonomagmatic processes associated with the 1.1 Ga mid-continent rift system. *Journal of Geophysical Research*, 98B: 13,997–14,013.

PAULO, A. & SALAMON, W., 1974. Przyczynek do znajomości złoża polimetalicznego w Starej Górze. [Contribution to the knowledge of polymetallic ore deposit in Stara Góra.] *Kwartalnik Geologiczny*, 18/2: 266–276, , {in Polish, English summary}.

PEARCE, J. A., HARRIS, N. B. W. & TINDLE, A. G., 1984. Trace element discrimination for the tectonic interpretation of granitic rocks. *Journal of Petrology*, 25: 956–983.

PIDGEON, R. T., 1992. Recrystallisation of oscillatory zoned zircon: some geochronological and petrological implications. *Contributions to Mineralogy and Petrology*, 110: 463–472

PIDGEON, R. T., NEMCHIN, A. A. & HITCHEN, G. J., 1998. Internal structures of zircons from Archean granites from the Darlin Range batholith: implications for zircon stability and the interpretation of zircon U-Pb ages. *Contributions to Mineralogy and Petrology*, 132: 288–299.

PIN, C., PUZIEWICZ, J. & DUTHOU, J. L., 1989. Ages and origin of a composite granitic massif in the Variscan belt: a Rb-Sr study of the Strzegom-Sobótka Massif, W Sudetes (Poland). *Neues Jahrbuch für Mineralogie, Abhandlungen*, 160: 71–82.

PUPIN, J. P., 1980. Zircon and granite petrology. *Contributions to Mineralogy and Petrology*, 73: 207–220.

PUPIN J. P., 1988. Granites as indicators in paleogeodynamics. *Rendiconti della Societa Italiana di Mineralogia e Petrologia,* 43–2: 237–262.

PUPIN, J. P. & TURCO, G., 1972. Une typologie originale du zircon accessoire. *Bulletin de la Société Française de Minéralogie et de Cristallographie* 95: 348–359.

SCHALTEGGER, U., FANNING, C. M., GUENTER, D., MAURIN, J. C., SCHULMANN, K. & GEBAUER, D., 1999. Growth, annealing and recrystallization of zircon and preservation of monazite in high-grade matamorphism: conventional and in-situ U-Pb isotope, cathodoluminescence and microchemical evidence. *Contributions to Mineralogy and Petrology*, 134: 186–201.

SKOWRONEK, A., STEFFAHN, K., 2000. The age of the Kauffung Limestones (W Sudetes, Poland) – a revision due to new discovery of microfossils. *Neues Jahrbuch für Geologie und Paläontologie, Monatshefte*, 2: 65–82.

SŁABY, E. & MARTIN, H. 2008. Mafic and Felsic Magma Interaction in Granites: the Hercynian Karkonosze Pluton (Sudetes, Bohemian Massif). *Journal of Petrology*, 49:

353–391.
STACEY, J. S. & KRAMERS, J. D., 1975. Approximation of terrestrial lead isotope evolution by a two-stage model. *Earth and Planetary Science Letters*, 26: 207–221.
TIMMERMANN, M., PARRISH, R. R., NOBLE, S. R. & KRYZA, R., 2000. New U-Pb monazite and zircon data from the Sudetes Mountains in SW Poland: evidence for a single-cycle Variscan orogeny. *Journal of the Geological Society, London*, 157: 265–268.
TURNIAK, K., HAŁAS, S. & WÓJTOWICZ, A., 2007. New K-Ar cooling ages of granitoids from the Strzegom–Sobótka Massif (SW Poland). *Geochronometria*, 27 (in press).
TURNIAK, K., TICHOMIROWA, M. & BOMBACH, K., 2005. Zircon Pb-evaporation ages of granitoids from the Strzegom–Sobótka Massif (SW Poland). *Mineralogical Society of Poland, Special Papers*, 25: 241–245.
TURNIAK, K., TICHOMIROWA, M. & BOMBACH, K., 2006. Pb-evaporation zircon ages of post tectonic granitoids from the Strzelin Massif (SW Poland). *Mineralogia Polonica, Special Papers*, 29: 212–215.
URBANEK, Z. & BARANOWSKI, Z., 1986. Revision of the age of the Radzimowice slates from the Góry Kaczawskie, Western Sudetes. *Annales Societatis Geologorum Poloniae*, 56, 3-4: 399–408.
WILLIAMS, I. S., 1998. U-Th-Pb geochronology by ion microprobe. *In*: McKibben, M. A., Shanks (III), W. C. & Ridley, W. I. (Eds), *Applications of microanalytical techniques to understanding mineralizing processes, Reviews in Economic Geology*, 7: 1–35.
WINCHESTER, J. A. & FLOYD, P. A., 1977. Geochemical discrimination of different magma series and their differentiation products using immobile elements. *Chemical Geology*, 20: 325–343.
ŻELAŹNIEWICZ, A., 2003. Postęp wiedzy o geologii krystaliniku Sudetów latach 1990–2003. [Developments in the geology of the crystalline basement of the West Sudetes in 1990–2003]. *In*: Ciężkowski, W., Wojewod, J. & Żelaźniewicz, A. (Eds), *Sudety Zachodnie: od wendu do czwartorzędu*. WIND, Wrocław: 7–16, {in Polish, English summary}.

Appendix 1

Chemical composition of the selected samples of granitoids, volcanic rocks and kersantites from the Żeleźniak Hill area

Sample	82/9 rhyo-dacite	125 trachy-andesite	5/10 trachy-andesite	79/2 trachy-andesite	23/9 rhyo-dacite	53 trachy-andesite	26 rhyo-dacite	23/5 monzo-granite	12 monzo-granite	5 monzo-granite	14 monzo-granite	C grano-diorite	85 monzo-granite	5/5 monzo-granite	WB102a grano-diorite	KH3/2 kersan-tite	KH3/1 kersan-tite
SiO_2	71.00	74.01	72.59	73.23	70.86	68.90	72.14	72.32	66.85	71.34	71.20	66.18	70.81	72.65	68.73	43.94	44.63
Al_2O_3	14.22	15.05	13.93	14.41	15.15	13.90	14.65	15.66	14.98	14.75	15.71	16.43	14.85	14.54	15.69	12.37	12.76
Fe_2O_3	2.66	1.32	2.49	1.40	2.60	1.66	2.26	2.21	2.52	2.50	2.67	3.94	2.18	2.38	2.76	8.67	8.63
MnO	0.89	0.050	0.022	0.013	0.63	0.026	0.114	0.074	0.080	0.039	0.088	0.034	0.052	0.032	0.030	0.392	0.200
MgO	0.34	0.25	0.86	0.62	0.55	1.05	0.25	0.45	1.39	0.85	0.61	1.53	0.58	0.45	0.96	7.31	8.89
CaO	1.50	0.18	1.11	0.94	1.45	2.05	1.09	0.13	2.53	1.61	0.20	2.32	1.01	0.29	3.52	7.21	7.47
Na_2O	1.63	3.24	3.53	3.63	3.61	2.88	2.26	2.34	1.57	3.70	3.35	4.07	4.14	3.48	4.21	1.62	1.86
K_2O	5.41	3.99	3.88	4.42	4.25	5.42	4.12	4.56	3.53	3.91	4.04	3.10	3.65	4.01	3.04	2.20	2.61
TiO_2	0.202	0.152	0.297	0.266	0.22	0.273	0.203	0.283	0.378	0.317	0.280	0.454	0.238	0.202	0.471	0.866	0.970
P_2O_5	0.10	0.10	0.14	0.12	0.12	0.11	0.10	0.10	0.11	0.13	0.13	0.27	0.11	0.11	0.13	0.26	0.39
LOI	2.77	1.87	1.41	1.27	1.18	4.08	3.20	2.16	5.65	1.07	1.91	2.00	1.64	1.97	0.62	13.69	10.18
suma	99.92	100.21	100.25	100.32	100.03	100.35	100.39	100.27	99.58	100.21	100.16	100.34	99.24	100.11	100.17	98.53	98.59
Sr	230	324	298	319	288	215	253	107	192	399	231	555	367	159	411	349	485
Y	18.9	17.6	11.0	12.6	20.7	14.1	21.6	17.3	13.7	11.8	19.4	18.1	16.2	12.7	15.9	20.0	21.5
Sc	5	4	5	4	5	4	4	5	6	4	6	5	4	4	7	28	27
Be	2	3	2	2	3	2	2	2	2	2	2	2	2	2	1	2	2
V	23	31	31	21	13	25	10	27	48	29	27	59	12	12	48	148	162
Cr	-20	-20	-20	-20	-20	155	-20	-20	22	-20	-20	-20	-20	-20	-20	148	162
Co	20	60	62	56	30	57	29	154	26	82	49	73	99	61	38	48	43
Ni	-20	-20	-20	-20	-20	194	-20	-20	-20	-20	-20	-20	-20	-20	-20	190	249
Cu	12	-10	60	146	-10	137	21	23	11	61	12	177	13	-10	-10	83	933
Zn	-30	-30	-30	35	-30	-30	487	189	46	80	167	-30	63	91	-30	94	159
Ga	16	16	15	19	18	17	19	21	22	24	23	26	22	18	19	13	15
Ge	0.9	1.2	1.5	1.0	1.2	0.9	1.8	3.0	3.8	1.2	1.4	2.0	1.4	1.2	2.0	0.9	0.7
As	18	19	11	66	39	11	7	27	127	12	29	17	6	10	-5	2580	1230
Rb	156	109	70	108	125	153	173	179	151	123	147	80	118	112	102	82	94
Zr	129	139	139	133	143	129	150	165	164	147	183	196	165	151	137	110	159
Nb	11.6	14.9	10.5	11.5	10.9	11.2	13.6	11.1	9.9	11.8	13.4	14.2	14.4	10.1	8.9	7.7	10.9
Mo	-2	-2	-2	2	-2	7	3	-2	3	-2	3	-2	-2	-2	-2	-2	-2
Ag	-0.5	-0.5	-0.5	-0.5	-0.5	-0.5	-0.5	-0.5	-0.5	-0.5	-0.5	-0.5	-0.5	-0.5	-0.5	-0.5	52.9
In	-0.1	-0.1	-0.1	-0.1	-0.1	-0.1	-0.1	-0.1	-0.1	-0.1	-0.1	-0.1	-0.1	-0.1	-0.1	-0.1	0.2
Sn	3	1	-1	1	2	2	9	3	-1	2	4	2	1	-1	4	2	2

Appendix 1, continued

Chemical composition of the selected samples of granitoids, volcanic rocks and kersantites from the Żeleźniak Hill area

Sample	82/9 rhyo-dacite	125 trachy-andesite	5/10 trachy-andesite	79/2 trachy-andesite	23/9 rhyo-dacite	53 trachy-andesite	26 rhyo-dacite	23/5 monzo-granite	12 monzo-granite	5 monzo-granite	14 monzo-granite	C grano-diorite	85 monzo-granite	5/5 monzo-granite	WB102a grano-diorite	KH3/2 kersan-tite	KH3/1 kersan-tite
Sb	1.1	1.6	1.6	1.0	2.6	1.1	4.2	4.0	7.0	2.3	4.4	3.8	1.5	1.1	-0.2	129	526
Cs	3.9	4.6	1.7	2.6	4.1	4.0	5.1	4.0	6.7	3.9	2.8	4.2	2.1	2.8	2.5	7.1	3.9
Ba	1100	993	980	990	1080	1200	1690	1150	432	1090	1170	1080	1170	940	782	731	856
La	36.2	59.3	22.9	32.1	50.7	39.6	49.4	59.1	31.1	40.7	64.5	28.1	60.0	47.6	19.9	22.8	28.8
Ce	66.9	99.9	37.2	57.1	89.5	69.2	83.4	111	54.7	71.0	115	54.0	97.2	82.4	42.9	46.2	57.2
Pr	6.20	8.80	4.45	5.17	8.26	6.39	8.24	9.87	4.98	6.42	10.7	5.55	8.91	8.05	5.01	5.46	6.70
Nd	22.6	29.6	13.0	19.0	30.9	23.6	27.2	35.1	19.6	24.3	39.8	21.8	34.9	26.8	18.3	22.3	28.0
Sm	4.21	4.46	2.36	3.49	5.39	4.06	4.43	5.38	3.69	4.16	6.55	4.21	5.67	3.77	3.63	4.26	5.23
Eu	0.817	0.840	0.726	0.836	1.04	0.676	1.09	0.697	0.885	1.11	1.09	1.40	1.13	0.748	1.03	1.22	1.51
Gd	3.20	3.62	1.89	2.55	4.01	3.38	3.05	4.31	3.02	3.13	5.08	3.68	4.43	2.94	2.78	4.23	4.98
Tb	0.50	0.51	0.31	0.38	0.62	0.49	0.55	0.56	0.48	0.42	0.71	0.51	0.71	0.43	0.47	0.69	0.77
Dy	3.02	2.89	1.82	2.13	3.53	2.56	3.32	3.10	2.67	2.22	3.77	3.11	3.85	2.20	2.71	3.70	4.09
Ho	0.61	0.56	0.36	0.39	0.67	0.49	0.66	0.63	0.48	0.39	0.68	0.63	0.68	0.43	0.54	0.74	0.78
Er	1.78	1.79	1.13	1.20	1.98	1.56	1.90	1.85	1.46	1.20	2.12	1.97	2.23	1.33	1.49	2.32	2.39
Tm	0.278	0.290	0.189	0.191	0.331	0.258	0.272	0.295	0.241	0.196	0.361	0.323	0.389	0.212	0.201	0.345	0.355
Yb	1.83	1.89	1.34	1.29	2.04	1.60	1.86	1.85	1.60	1.35	2.15	2.18	2.30	1.40	1.39	2.10	2.19
Lu	0.260	0.273	0.189	0.185	0.296	0.233	0.268	0.270	0.211	0.196	0.309	0.351	0.319	0.213	0.194	0.323	0.311
Hf	3.8	4.7	4.0	3.8	4.6	4.0	4.2	5.1	4.9	4.6	6.0	5.3	5.5	4.0	3.6	3.0	4.4
Ta	1.17	1.50	1.21	1.21	1.22	1.27	1.23	1.44	1.07	1.26	1.57	1.24	1.65	1.15	0.92	0.60	0.72
W	130	404	436	473	214	476	204	1080	193	610	391	504	704	422	271	60.7	33.5
Tl	1.74	0.09	0.12	0.81	0.58	0.87	1.65	0.78	0.86	0.73	0.99	0.15	0.38	0.57	0.43	0.32	0.30
Pb	11	-5	-5	23	20	10	47	8	25	24	118	-5	29	38	12	23	4610
Bi	0.4	0.1	0.2	0.9	-0.1	0.9	0.4	0.3	-0.1	0.7	0.4	0.2	-0.1	2.8	0.1	0.7	146
Th	15.4	17.5	13.2	15.3	17.9	16.8	17.6	22.9	16.4	19.1	23.5	15.5	23.2	18.7	7.77	6.09	6.76
U	2.79	2.29	2.21	4.08	4.93	5.02	4.44	2.71	5.68	2.63	4.75	3.70	5.0	4.82	2.23	1.33	1.50

Appendix 2

Summary of SHRIMP U-Pb zircon data for sample 14

Grain spots	(1) % $^{206}Pb_c$	U (ppm)	Th (ppm)	$^{232}Th/^{238}U$	$^{206}Pb^*$ (ppm)	Total $^{238}U/^{206}Pb$ ± %	Total $^{207}Pb/^{206}Pb$ ± %	(1) $^{206}Pb^*/^{238}U$ ± %	(1) $^{206}Pb^*/^{238}U$ age
1.1	-	542	311	0.59	23.6	19.75 ± 0.62	0.05268 ± 1.5	0.05064 ± 0.63	318.4 ± 2.0
2.1	0.12	547	274	0.52	23.6	19.93 ± 0.64	0.05368 ± 1.4	0.05011 ± 0.65	315.2 ± 2.0
3.1	0.07	562	379	0.70	24.5	19.66 ± 0.64	0.05337 ± 1.4	0.05082 ± 0.78	319.5 ± 2.0
5.1	0.31	313	140	0.46	13.2	20.37 ± 0.76	0.0550 ± 1.9	0.04894 ± 0.67	308.0 ± 2.4
6.1	-	512	385	0.78	22.2	19.80 ± 0.65	0.05240 ± 1.5	0.05052 ± 0.87	317.7 ± 2.1
7.1	0.02	309	124	0.41	13.2	20.07 ± 0.85	0.0528 ± 2.0	0.04981 ± 0.87	313.4 ± 2.6
8.1	0.12	655	474	0.75	27.8	20.19 ± 0.61	0.05355 ± 1.3	0.04946 ± 0.62	311.2 ± 1.9
9.1	0.22	580	309	0.55	25.2	19.76 ± 0.62	0.05449 ± 1.3	0.05049 ± 0.64	317.5 ± 2.0
10.1	2.01	628	325	0.53	24.3	22.21 ± 0.70	0.06794 ± 1.3	0.04413 ± 0.72	278.4 ± 2.0
11.1	-	309	130	0.44	13.3	19.90 ± 0.76	0.05258 ± 1.8	0.05026 ± 0.77	316.1 ± 2.4
12.1	0.80	403	184	0.47	17.6	19.67 ± 0.90	0.05913 ± 1.5	0.05044 ± 0.92	317.3 ± 2.8
13.1	0.05	603	275	0.47	25.8	20.03 ± 0.64	0.05305 ± 1.3	0.04989 ± 0.65	313.9 ± 2.0
14.1	0.03	195	92	0.49	8.48	19.71 ± 0.89	0.0530 ± 2.4	0.05071 ± 0.91	318.9 ± 2.8
15.1	0.02	447	233	0.54	19.4	19.75 ± 0.68	0.05290 ± 1.6	0.05062 ± 0.70	318.4 ± 2.2
16.1	0.28	274	216	0.82	11.7	20.05 ± 0.81	0.0549 ± 2.0	0.04975 ± 0.83	313.0 ± 2.5
17.1	0.02	501	292	0.60	21.7	19.86 ± 0.91	0.05291 ± 1.4	0.05035 ± 0.93	316.7 ± 2.9

Errors are 1 –sigma; Pb_c and Pb* indicate the common and radiogenic portions, respectively.
Error in standard calibration was 0.18% (not included in above errors but required when comparing data from different mounts)
Common Pb corrected by assuming $^{206}Pb/^{238}U$ - $^{207}Pb/^{235}U$ age-concordance

Grain spots	(1) % $^{206}Pb_c$	U (ppm)	Th (ppm)	$^{232}Th/^{238}U$	$^{206}Pb^*$ (ppm)	Total $^{238}U/^{206}Pb$ ±%	Total $^{207}Pb/^{206}Pb$ ± %	(1) $^{207}Pb^*/^{206}Pb^*$ ±%	(1) $^{206}Pb^*/^{238}U$ ± %	(1) $^{207}Pb^*/^{235}U$ ± %	$^{206}Pb/^{238}U$ age	$^{207}Pb/^{206}Pb$ age	err corr
4.1	1.09	298	219	0.76	14.5	17.64 ± 1.1	0.0623 ± 2.5	0.0572 ± 2.5	0.05632 ± 1.1	0.444 ± 2.7	353.2 ± 3.7	500 ± 55	0.402
4.2	1.30	448	216	0.50	28.6	13.440 ± 0.64	0.06665 ± 3.3	0.0611 ± 3.3	0.07389 ± 0.68	0.622 ± 3.3	459.5 ± 3.0	642 ± 70	0.204
11.2	2.94	642	927	1.49	248	2.223 ± 0.51	0.17516 ± 0.27	0.1742 ± 0.3	0.4493 ± 0.51	10.790 ± 0.58	2 392 ± 10	2 598.2 ± 4.6	0.883

Errors are 1 –sigma; Pb_c and Pb* indicate the common and radiogenic portions, respectively.
Error in standard calibration was 0.18% (not included in above errors but required when comparing data from different mounts)
Common Pb corrected using measured ^{204}Pb

Appendix 3

Summary of SHRIMP U-Pb zircon data for sample 26

Grain spots	(1) % $^{206}Pb_c$	U (ppm)	Th (ppm)	$^{232}Th/^{238}U$	$^{206}Pb^*$ (ppm)	Total $^{238}U/^{206}Pb \pm$%	Total $^{207}Pb/^{206}Pb \pm$%	(1) $^{206}Pb^*/^{238}U \pm$%	(1) $^{206}Pb/^{238}U$age
1.1	0.29	147	57	0.40	6.20	20.35±1.0	0.0548±2.7	0.0490±1.0	308.3±3.1
2.1	12.78	1092	539	0.51	45.5	20.63±0.53	0.15405±0.61	0.0423±0.55	267.0±1.4±
3.1	6.20	583	293	0.52	22.2	22.53±0.62	0.1012±1.2	0.0416±0.64	263.0±1.7
4.1	1.91	358	177	0.51	15.1	20.38±0.71	0.0677±1.5	0.0481±0.73	303.0±2.1
5.1	14.42	1248	613	0.51	54.0	19.84±0.51	0.1673±0.77	0.0431±0.55	272.2±1.5
6.1	0.38	101	38	0.39	4.35	20.03±1.2	0.0556±3.1	0.0497±1.23	312.9±3.8
7.1	0.05	265	324	1.26	11.4	20.01±1.0	0.0530±1.9	0.0499±1.10	314.1±3.3
8.1	3.39	1141	440	0.40	43.5	22.53±0.53	0.07886±0.86	0.0429±0.54	270.7±1.4
9.1	0.19	577	422	0.76	25.0	19.85±0.62	0.05424±1.3	0.0503±0.63	316.3±2.0
10.1	41.99	1717	1356	0.82	86.2	17.12±0.48	0.3861±0.75	0.0339±0.79	214.8±1.7
11.1	19.61	1106	520	0.49	55.0	17.27±0.51	0.2097±1.1	0.0465±0.63	293.3±1.8
11.2	0.09	384	100	0.27	25.9	12.76±0.66	0.05756±1.2	0.0783±0.68	486.0±3.2
12.1	-	586	426	0.75	25.0	20.18±0.61	0.05100±1.3	0.0497±0.63	312.4±1.9
13.1	0.14	240	136	0.58	10.3	19.94±1.2	0.0538±2.0	0.0501±1.23	315.1±3.8
15.1	2.02	591	266	0.47	24.3	20.84±0.63	0.0685±2.2	0.0470±0.66	296.1±1.9
16.1	0.07	565	313	0.57	24.2	20.05±0.79	0.05320±1.4	0.0499±0.81	313.6±2.5
17.1	0.21	675	550	0.84	29.4	19.72±0.60	0.05446±1.2	0.0506±0.61	318.1±1.9

Errors are 1 –sigma; Pb_c and Pb^* indicate the common and radiogenic portions, respectively.
Error in standard calibration was 0.18% (not included in above errors but required when comparing data from different mounts)
Common Pb corrected by assuming $^{206}Pb/^{238}U$ - $^{207}Pb/^{235}U$ age-concordance

Grain spots	(1) % $^{206}Pb_c$	U (ppm)	Th (ppm)	$^{232}Th/^{238}U$	$^{206}Pb^*$ (ppm)	Total $^{238}U/^{206}Pb$ ±%	Total $^{207}Pb/^{206}Pb$ ± %	(1) $^{207}Pb^*/^{206}Pb^*$ ±%	(1) $^{206}Pb^*/^{238}U$ ± %	(1) $^{207}Pb^*/^{235}U$ ± %	$^{206}Pb/^{238}U$ age	$^{207}Pb/^{206}Pb$ age	err corr
14.1	1.16	143	74	0.53	43.9	2.806±0.81	0.12947±0.75	0.1274±0.75	0.3555±0.81	6.247±1.1	1,961 ± 14	2,063 ± 13	.733

Errors are 1 –sigma; Pb_c and Pb* indicate the common and radiogenic portions, respectively.
Error in standard calibration was 0.18% (not included in above errors but required when comparing data from different mounts)
Common Pb corrected using measured ^{204}Pb